# Fabrication of metallic nanostructures by atomic force microscopy nanomachining and lift-off process

Ju-Hung Hsu, Chun-Yu Lin, and Heh-Nan Lin[a)]
*Department of Materials Science and Engineering, National Tsing Hua University, Hsinchu 300, Taiwan*

(Received 3 June 2004; accepted 20 September 2004; published 17 November 2004)

We report the fabrication of metallic nanostructures by atomic force microscopy nanomachining on a thin resist and subsequent metal coating and lift-off. Nanodots with a size of 70 nm, nanowires with a width of 120 nm, and nanoelectrodes with a gap of 50 nm have been successfully created. Theoretical estimates of the minimum force for a satisfactory lift-off are also given and found to be consistent with the experimental value. The present work demonstrates the feasibility and effectiveness of using a single-layer resist in comparison with a two-layer resist. © *2004 American Vacuum Society.* [DOI: 10.1116/1.1815314]

## I. INTRODUCTION

Scanning probe lithography has been used extensively in recent years for the fabrication of nanostructures and nanodevices.[1] Among the various techniques, atomic force microscopy (AFM) nanomachining has been adopted since the early years due to its ease of operation and applicability on insulating substrates.[2,3] By controlling the contact force between the AFM tip and the sample, desired nanostructures can be created. In this simplest scheme, however, the tip is vulnerable and not suitable for long time use, especially on hard materials.

By incorporating the notion of optical or electron-beam lithography, modifications of AFM nanomachining have consequently appeared. With the use of a thin resist on the substrate, the so-called one-layer approach, holes or grooves can be first generated by indenting or plowing the tip into the resist.[4–6] With subsequent chemical etching and resist removal, nanopatterns are produced on the substrate. Nevertheless, the created nanostructures are etched patterns and thus negative.[4–6] Protruding and positive metallic nanostructures have so far been generated by electrochemical deposition.[7] A different version of electrochemical deposition has also been realized by scratching the native oxide layer of a silicon substrate with a diamond-coated tip.[8] Creation of positive metallic nanostructures with the one-layer approach by a combination of AFM nanomachining, metal coating, and lift-off, has been absent in the literature to our knowledge.

The one-layer approach has a claimed disadvantage that the tip still experiences damage. A further modification is the use of a two-layer resist. In this methodology, the nanomachining is performed on the top layer and the tip damage is therefore minimal since the second layer is a soft material. With following chemical etching (into the second layer), coating, and lift-off, metallic nanostructures have been successfully generated.[9–11] A variation that utilizes a top metal layer and AFM nano-oxidation to construct openings on the metal layer for subsequent etching has also appeared.[12] As the two-layer approach is more complicated, it is desirable that the one-layer approach can be realized by standard lift-off process. In this article, the goal is achieved and metallic nanostructures including nanodots, nanowires, and nanoelectrodes are successfully fabricated. Theoretical considerations of the indentation force are also explored.

## II. EXPERIMENT

The experimental procedure is show in Fig. 1. A solution of 1.25 wt % poly(methylmethacrylate) (PMMA) (molecular weight 965 000 g) in chlorobenzene was spin-coated on a sapphire or silicon substrate, which was cleaned in an ultrasonic bath of acetone prior to coating. After a 30 min soft baking at 150 °C, the PMMA film was produced and also free of pin-holes. The thickness and the root-mean-square roughness were around 50 and 0.25 nm, respectively, as determined by AFM measurement.

A commercial AFM (Smena-B, NT-MDT, Russia) and rectangular silicon probes (NSC15, MikroMasch, Russia) with a tip diameter of 20 nm were employed for the experiment. The probes had listed values of 40 N/m for the spring constant and 325 kHz for the resonant frequency. Nevertheless, the measured resonant frequencies were far below the listed value. Since the spring constant is proportional to the square of the resonant frequency for a rectangular probe, the corrected value of 32.5 N/m, which corresponded to a resonant frequency of 293 kHz, was used for force calculation. The scanner was calibrated by a standard grating (TGZ02, MikroMasch, Russia) in three directions, and the detector sensitivity was characterized from a force–distance curve on a silicon substrate. The force was determined from a force–distance curve on the PMMA film. (Note that the detector sensitivity is probe-dependent and the same probe should be used in related measurements.)

The AFM was operated in the tapping mode for imaging. The contact mode operation was not adopted since the PMMA surface was frequently damaged due to the large spring constant of the employed probes. Each indentation was realized by moving the scanner (to which the tip was attached) in the vertical ($z$ axis) direction toward the sample. A desired pattern of holes was created by locating the tip on

[a)]Author to whom correspondence should be addressed; electronic mail: hnlin@mx.nthu.edu.tw

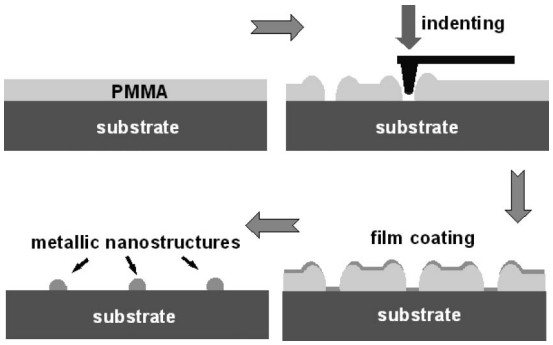


FIG. 1. Schematic diagram of the experimental procedure.

designated positions controlled by the software. A straight groove could also be produced by indenting and moving the tip along a straight line. A gold or copper film was then coated on the sample by ion sputtering or electron-beam evaporation, respectively. The sample was finally soaked in acetone to remove the PMMA and dried by nitrogen gas. All nanodots (nanowires) presented in the following were produced on sapphire (silicon) substrates.

## III. RESULTS

As can be imagined, the lift-off process will fail unless the indented hole reaches the substrate in an indentation. A large force is required from this aspect. On the other hand, the hole gets larger when the force is higher. Various scanner moving distances were tested and the minimum distance for a successful lift-off was found to be around 180 nm. Using this value, which corresponded to an indentation force of 3.8 $\mu$N (see Sec. IV), a nanohole array was generated on the PMMA film on a sapphire substrate and the AFM image is shown in Fig. 2(a). The pile-up around each hole is apparent, which is similar to those reported previously.[2,5,6,8,10] After coating a 10-nm-thick gold film and removing the PMMA, a gold nanodot array with a smallest dot size of around 70 nm was fabricated and the result is shown in Fig. 2(b).

In addition to regular arrays, complicated dot patterns were also constructed. In Fig. 2(c), the scanning electron microscope (SEM) image of a pattern "NANO" is presented.[13] The result demonstrates the ease and effectiveness of the present method to generate nanoscale patterns. Similar nanodots were also obtained on silicon substrates, indicating little influence of using different substrates. With the use of thinner resists, the creation of smaller nanodots should be feasible. The minimum dot size should be comparable to the tip diameter, which is around 20 nm and can be considered as the resolution of AFM nanomachining.

With the use of the 3.8 $\mu$N indentation force, the tip damage was minimal even after hundreds of indentations. The SEM images of a new tip, the tip after 625 indentations, and the resultant gold nanodot array are shown in Fig. 3.[13] Furthermore, it was also verified that more than 5000 nanodots of sizes around 100 nm could be fabricated by a single tip. The influence of the indentation force on the dot size has also been explored. The results for four different forces of 4.3, 5.6, 6.8, and 8.1 $\mu$N (top to bottom for every two rows) are shown in Fig. 4(a).[13] Including previous results for 3.8 $\mu$N, the relationships between the dot dimensions in both axes

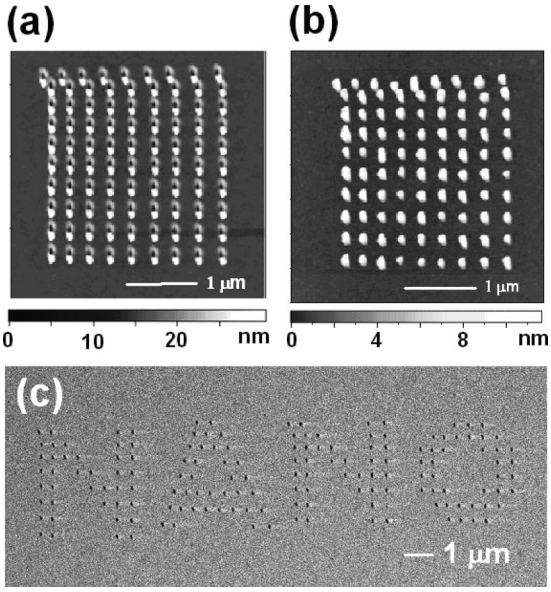


FIG. 2. AFM images of (a) a nanohole array on PMMA and (b) the corresponding gold nanodot array after lift-off. (c) SEM image of a gold nanodot pattern "NANO" (Ref. 13). Note that all nanodots were created on sapphire substrates.

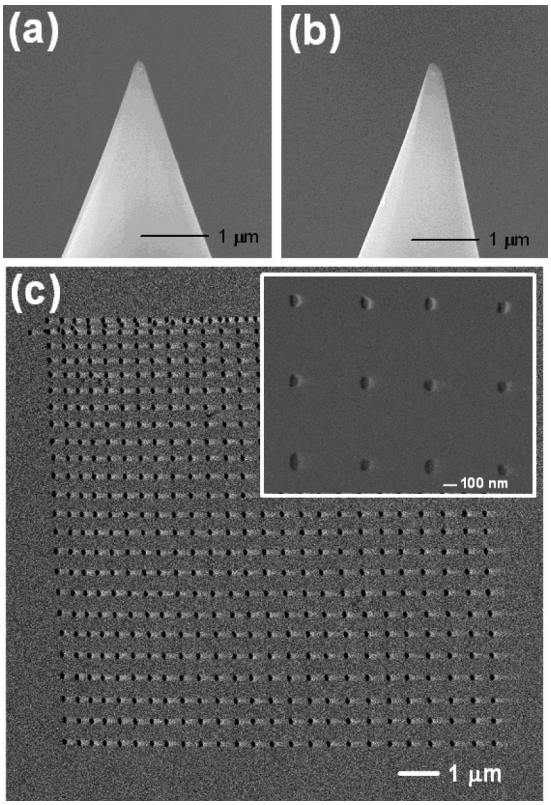


FIG. 3. SEM images of (a) a new tip, (b) the same tip after 625 indentations, and (c) the resultant $25\times25$ gold nanodot array and a zoomed image of the nanodots (Ref. 13).

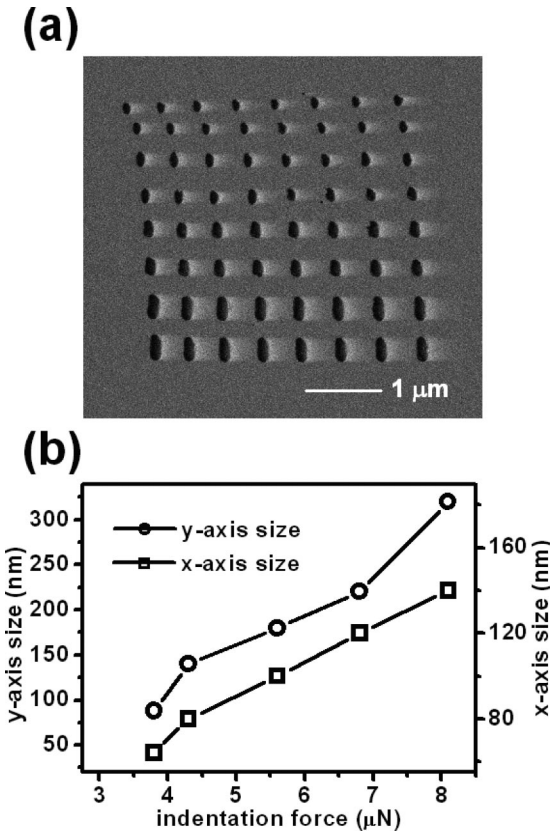


FIG. 4. (a) SEM image of a gold nanodot array created by four different forces of 4.3, 5.6, 6.8, and 8.1 $\mu$N (top to bottom for every two rows), and (b) the relationships between the dot dimensions in both axes and the indentation force.

and the indentation force are plotted in Fig. 4(b). It is interesting to note that the dots become elongated in one direction under high forces. The elongation has been confirmed to be along the cantilever axis and is apparently caused by the large cantilever bending at a high load.

In addition to the fabrication of nanodots, metallic nanowires were also created by generating nanogrooves on the PMMA and subsequent lift-off. For demonstration, a copper nanowire with a width of around 120 nm was produced on a silicon substrate after evaporating a 4-nm-thick gold film and a 20-nm-thick copper film, and the AFM image is shown in Fig. 5(a). To verify the electric conduction of the wire, copper pads were also fabricated concurrently by scratching the PMMA film with a needle before the AFM nanomachining.

The current–voltage relationship was measured in a two-point geometry with the use of a Keithley 2400 source-measure unit and the result is plotted in Fig. 5(b). The linear relationship, which corresponds to a resistance of 2.54 k$\Omega$, ascertains the good conductive behavior of the wire. By assuming the wire with a length, a width, and a height of 4.7 $\mu$m, 120 nm, and 24 nm, respectively, the calculated resistivity is $1.56\times10^{-4}$ $\Omega$ cm. This value is two orders of magnitude higher than the bulk resistivity of copper. In comparison with a reported resistivity of $1.71\times10^{-5}$ $\Omega$ cm for a single-crystalline copper nanowire with a diameter of 60 nm,[14] our higher value is not unexpected since the present

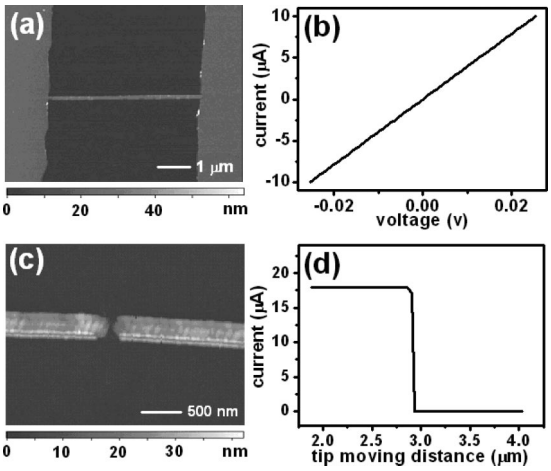


FIG. 5. (a) AFM image of a copper nanowire with a width of 120 nm on a silicon substrate, and (b) the corresponding $I-V$ curve that shows a resistance of 2.54 k$\Omega$. (c) A pair of nanoelectrodes created by cutting a different nanowire, and (d) the simultaneously obtained relationship of current vs tip moving distance.

wire is polycrystalline. In addition, it was found in the same work that the resistivity of a copper nanowire changed by orders of magnitude due to oxidation,[14] which is also a plausible explanation for our higher resistivity.

With a further effort, nanoelectrodes were also fabricated by direct cutting of a nanowire with the AFM tip. A pair of nanoelectrodes with a gap of around 50 nm was produced by cutting a different nanowire at a cutting speed of 0.2 $\mu$m/s,[15] and the image is shown Fig. 5(c). Simultaneous current versus tip moving distance during cutting is also plotted in Fig. 5(d), and the zero current after cutting certifies that the nanowire was cut off completely. The present method of producing nanowires and nanoelectrodes is again simple and effective.

## IV. FORCE CALCULATION

The indentation force has a significant influence on the dot size as has already been shown and it is important to accurately determine its magnitude. The force is simply equal to the product of the tip spring constant and the tip deflection. In Fig. 6, the force and the vibration amplitude are plotted against the $z$-axis position. (A positive position means that the scanner is away from the sample and the scanner moving distance in an indentation is relative to the origin.) The indentation process is also exemplified in Fig. 6. When the scanner moves, the tip vibration amplitude decreases and reaches zero at a moving distance of $w$, which is dependent on the choice of imaging setpoint. The tip bending begins after that and also indents into the PMMA film. Since the minimum scanner moving distance for a successful lift-off is around 180 nm as mentioned previously, the force amounts to 3.8 $\mu$N from Fig. 6. Different forces corresponding to different moving distances can also be determined directly from Fig. 6.

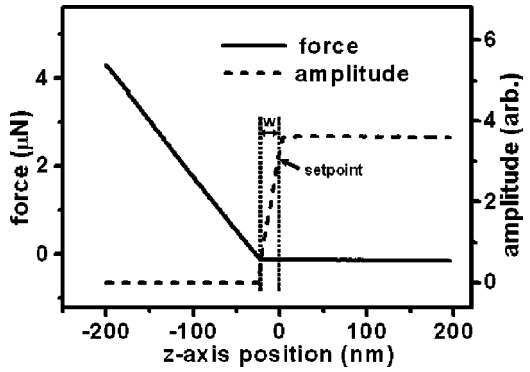


FIG. 6. Plots of indentation force (i.e., the product of spring constant and deflection) and tip vibration amplitude vs scanner *z*-axis position.

For a better understanding of the indentation force, it is instructive to use a simple argument to estimate the minimum force. As has already been explained earlier, it is clear that in an indentation,

$$D = w + \delta + d = w + \delta + \frac{F}{k}, \tag{1}$$

where $D$ is the scanner moving distance toward the sample, $\delta$ the penetration depth, $d$ the tip deflection (bending), $F$ the indentation force, and $k$ the spring constant. Suppose at the minimum moving distance ($\sim$180 nm), the tip just indents to the bottom of the PMMA. With $w$ and $\delta$ equal to 30 (from Fig. 6) and 50 nm (film thickness), respectively, the minimum force is therefore 3.25 $\mu$N. This value is close to but slightly less than the experimental value as expected. The calculation indicates that the 180 nm is a suitable distance for the fabrication although a shorter distance should still be feasible from the calculation.

There is also a theoretical formula that can be used to estimate the minimum force. In Fig. 6, the force and the distance have a linear relationship after the indentation begins. From the Sneddon formulism of indentation, the linear behavior is the signature of a rigid cylindrical punch with the following relationship:[16]

$$F = \frac{2E}{1-\nu^2} a\delta, \tag{2}$$

where $E$ is the Young's modulus, $\nu$ the Poisson's ratio, $a$ the radius of the cylindrical indenter, $\delta$ the penetration depth. With the parameters $3\times10^9$ Pa for $E$, 0.35 for $\nu$,[17] 10 nm for $a$, and 50 nm for $\delta$, the calculated minimum force is 3.42 $\mu$N. This value is again in good agreement with the experimental value.

## V. CONCLUSION

To summarize, we have presented a method to fabricate metallic nanostructures by a combination of AFM nanomachining and standard lift-off process. By controlling the force of an AFM tip on a thin resist, nanoscale holes and grooves are first created. By coating a metal film and performing the lift-off process, metallic nanodots with a smallest size of 70 nm and nanowires with a width of 120 nm are successfully fabricated. Furthermore, nanoelectrodes with a gap of around 50 nm are also produced by cutting a nanowire with the tip. Theoretical calculations for the minimum indentation force have been elaborated and are in good agreement with the experimental value. In addition, tip wear has been proven minimal even after thousands of indentations, which is opposed to the common impression of high risk of tip damage for the one-layer approach.

## ACKNOWLEDGMENTS

This work was supported by the Ministry of Education, Program of Academic Excellence under Grant No. 91-E-FA04-1-4 and the National Science Council under Grant No. 92-2120-E-007-005.

[1] H. T. Soh, K. W. Guarini, and C. F. Quate, *Scanning Probe Lithography* (Kluwer, Boston, 2001).
[2] X. Jin and W. N. Unertl, Appl. Phys. Lett. **61**, 657 (1992).
[3] Y. Kim and C. M. Lieber, Science **257**, 375 (1992).
[4] M. Wendel, S. Kühn, H. Lorenz, J. P. Kotthaus, and M. Holland, Appl. Phys. Lett. **65**, 1775 (1994).
[5] B. Klehn and U. Kunze, J. Appl. Phys. **88**, 3897 (1999).
[6] K. Wiesauer and G. Springholz, J. Appl. Phys. **88**, 7289 (2000).
[7] L. A. Porter, Jr., A. E. Ribbe, and J. M. Buriak, Nano Lett. **3**, 1043 (2003).
[8] L. Santinacci, T. Djenizian, and P. Schmuki, Appl. Phys. Lett. **79**, 1882 (2001).
[9] L. L. Sohn and R. L. Willett, Appl. Phys. Lett. **67**, 1552 (1995).
[10] V. Bouchiat and D. Esteve, Appl. Phys. Lett. **69**, 3098 (1996).
[11] S. Hu, A. Hamidi, S. Altmeyer, T. Köster, B. Spangenberg, and H. Kurz, J. Vac. Sci. Technol. B **16**, 2822 (1998).
[12] M. Rolandi, C. F. Quate, and H. Dai, Adv. Mater. (Weinheim, Ger.) **14**, 191 (2002).
[13] Note that the gold nanodots appear dark on sapphire in the SEM images.
[14] M. E. Toimil Molares, E. M. Höhberger, C. Schaeflein, R. H. Blick, R. Neumann, and C. Trautmann, Appl. Phys. Lett. **82**, 2139 (2003).
[15] It should be noted that the cutting speed has a strong effect on the shape of nanoelectrodes. A slow speed usually generates a pair of curved electrodes.
[16] I. N. Sneddon, Int. J. Eng. Sci. **3**, 47 (1965). The employed NSC 15 is a conical tip with a diameter of 20 nm and a half angle of 10°. The approximation of a cylindrical punch is not an accurate one but still plausible since the penetration depth is only 50 nm.
[17] The Young's modulus for PMMA is from R. J. Young and P. A. Lovell, *Introduction to Polymers* (Chapman and Hall, New York, 1991), p. 420. The Poisson's ratio has a minor effect in the calculation and is taken as that of polystyrene.